

Original Article

Impact of burn priming on immune and metabolic functions of whole Liver in a rat cecal ligation and puncture model

John SA Mattick¹, Qian Yang¹, Mehmet A Orman¹, Marianthi G Ierapetritou¹, Francois Berthiaume³, Stephen C Gale⁴, Ioannis P Androulakis^{1,3}

¹Chemical and Biochemical Engineering Department, Rutgers, the State University of New Jersey, Piscataway, NJ, 08854, USA; ²BioMaPS Institute for Quantitative Biology, Rutgers University, Piscataway, NJ, 08854, USA;

³Biomedical Engineering Department, Rutgers, the State University of New Jersey, Piscataway, NJ, 08854, USA;

⁴Department of Surgery, RWJMS/UMDNJ, New Brunswick, NJ, 08901, USA

Received December 12, 2012; Accepted January 10, 2013; Epub January 24, 2013; Published January 30, 2013

Abstract: Previously, we have shown that systemic insults in single injury models produced immunosuppressive effects in burn, and a strong acute phase response in sepsis through hepatic gene expression. In order to investigate the implications of these effects on a combined injury, a double hit model was explored to mimic the progression of clinical burn-sepsis. Rodents were subjected to a 20% total body surface area (TSA) full-thickness burn injury, and 48 hours later underwent cecal ligation and puncture (CLP) to induce sepsis. Pathways related to innate immune signaling through cytokines and NF-KB were co regulated with xenobiotic metabolism genes and acute phase protein genes, and that these genes were suppressed early, and then activated. Furthermore, we were able to identify that, in addition to amino acid metabolism, pyruvate metabolism, fatty acid metabolism and NRF-2 mediated oxidative stress genes were down regulated over the time course. Overall, these observed trends within the double hit burn-sepsis model represent unique immune and metabolic pathways and dynamics not found in either injury, including an early suppression followed by overreaction of pro inflammatory mediators, and an increase in amino acid metabolism at the expense of central carbon pathways.

Keywords: Sepsis, burns, microarray analysis, RT-PCR analysis, liver

Introduction

After significant systemic injury, such as burn trauma, an immune response is triggered with an initial pro-inflammatory and subsequent anti-inflammatory phase. The innate immune system is critical to these mammalian immune responses and is tasked both with clearing foreign pathogens/debris and promoting wound healing. Interestingly, evidence further suggests that a series of *multiple* injuries, in succession, can produce an exaggerated and more pathologic immune response than after individual insults [1]. Experimental burn injury, followed by sepsis induced by cecal ligation and puncture, is a common model used to mimic this “double hit phenomenon,” as burn trauma is known to induce profound inflammation with subsequent immunosuppression and therefore

increased susceptibility to polymicrobial sepsis [2, 3]. Mechanistically, it is believed that burns induce an inflammatory response, followed by an anti inflammatory wound healing response that dominates the recovery phase [4]. This anti inflammatory state is believed to increase the severity of subsequent septic challenges by impeding the immune response [5, 6], which results in either overwhelming infection or a *hyperinflammatory* response [7]. In either setting, the end result is often multiple organ failure and, ultimately, death.

In the setting of inflammation and sepsis, the liver is at the crossroads of innate immune responses and systemic metabolic shifts [8], and therefore, examining hepatic metabolism is useful to characterize the systemic response of an immunocompromised host. With a rodent

model of burn inflammation and subsequent cecal ligation and puncture (CLP) [9], the effects of burn injury on the host response to infection can be studied longitudinally. Previously, we have used a similar methodology to conduct studies of the longitudinal responses of both burn and infection independently, with an emphasis on both the first 24 hours of the acute phase injury, and the long term recovery response out to 8 days [10-12]. We observed that although both burn and CLP induce an inflammatory response, burn appears to promote an anti inflammatory state after 24 hours [12] with toll-like receptor production for recognizing infection [13], while CLP creates strong, persistent acute pro inflammatory response. By combining these injuries into a two-hit model, we aim to characterize the net response of a host that is in an anti inflammatory state due to a prior burn injury [12] when it is subject to the pro inflammatory stimulus that is CLP [11]. Furthermore, we aim to reconcile the differences in metabolic changes that were observed in both the single burn and CLP injuries by characterizing the mechanisms by which they interact in order to create the hyper metabolic conditions that plague the clinical occurrences of burn-sepsis that this animal model aims to mimic.

The complexity and diversity of the hepatic metabolic response to injury, necessitates a comprehensive and efficient analysis which can be accomplished using functional genomics. These techniques allow a wide subset of transcriptional responses and metabolic pathways to be characterized ranging from fatty acid metabolism to innate immune protein synthesis. Because the liver simultaneously manages both metabolic changes and proinflammatory signaling it is critical to characterize and interpret these responses in parallel. Significant Analysis of Microarrays (SAM) can be utilized [14] to determine significantly varying genes following injury by using multiple gene-specific t-tests to verify the significance of the observed fold changes. Subsequent Ingenuity Pathway Analysis (IPA) can then be used to identify relevant pathways that are different between groups. By integrating these techniques, as shown in **Figure 1**, the present study aims to characterize the long term functional and dynamic differences that are created when burn injury serves as a priming mechanism for a subsequent septic insult.

In order to analyze the maximum number of genes possible in the hepatic response, microarray chips were used to simultaneously measure mRNA levels of approximately 31,000 genes. In order to confirm that the trends we measure from the microarray samples are real experimentally, a small subset of genes was identified for further RT-PCR analysis, in order to confirm trends found in the microarray probe sets. Genes were selected that showed significant differences between injury conditions, and which were as representative as possible of the wide array of genes we aimed to observe. Therefore, genes that were selected include metabolite transporters, metabolic enzymes, pro inflammatory transcription factors, acute phase proteins, and signaling molecules. Furthermore, genes were selected at both short and long term time points, in order to increase confidence in the accuracy of the microarray results throughout the experimental period.

Materials and methods

Animal model

Male Sprague-Dawley rats (Charles River Labs, Wilmington, MA) weighing 150-200g were utilized. The animals were housed in a temperature-controlled environment (25°C) with a 12-hour light-dark cycle and provided water and standard chow *ad libitum*. All experimental procedures were carried out in accordance with National Research Council guidelines and approved by the Rutgers University Animal Care and Facilities Committee.

A systemic hypermetabolic response was induced by applying a full-thickness burn on an area of the dorsal skin corresponding to 20% of the total body surface area (TBSA) with 100% survival, no evidence of systemic hypoperfusion and no significant alterations on feeding patterns as performed previously [12]. Briefly, animals were shaved in the dorsal abdominal area and immersed in water at 100°C for 10 seconds to produce a full-thickness 20% TBSA scald injury.

The septic insult was induced by applying CLP treatment 48 hours post burn treatment, using the same methods previously employed by our lab for single injury CLP animals [10, 15]. Briefly, the cecum of each rat was exposed and ligated

Microarray analysis in liver following burn and CLP

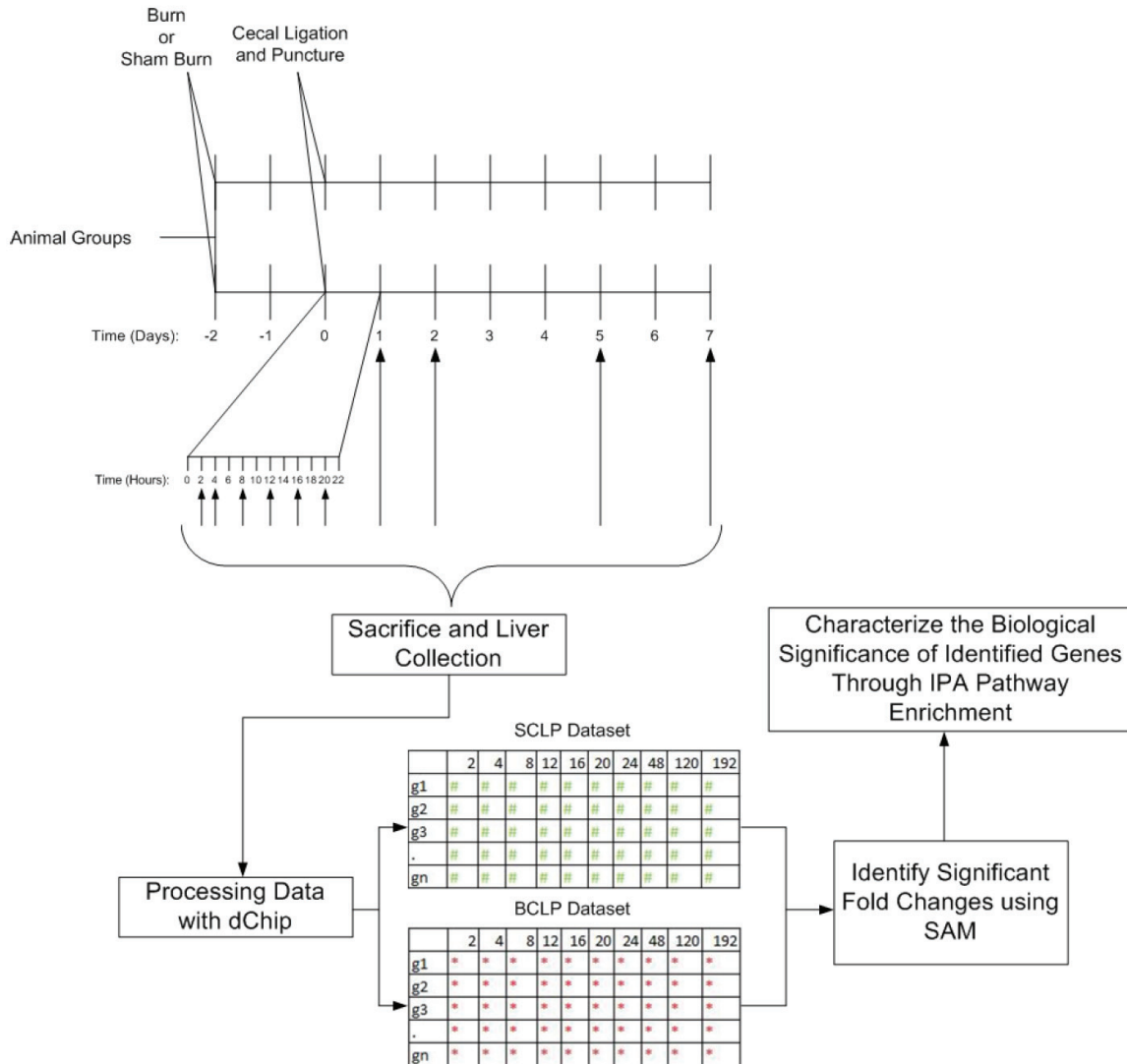


Figure 1. Schematic Overview of the Experimental Design. Animals were first subjected to burn or sham burn treatments, and then 48 hours later, were subjected to cecal ligation and puncture. Sacrifice occurred at 2, 4, 8, 12, 16, 20, 24, 48, 120, and 192 hours post CLP. Microarray data from the liver was preprocessed using dChip software, and then compared using SAM (Statistical Analysis of Microarrays) to determine genes with significantly altered expression. This subset of genes was then processed using Ingenuity Pathway Analysis enrichment software in order to characterize the biological differences between the two injury models.

just below the ileocecal valve, then punctured 4 times with a 20-gauge needle and replaced in the peritoneum once extrusions were observed.

Animals were sacrificed (starting at 9am) at different time points (2, 4, 8, 12, 16, 20, 24, 48, 120 and 192 hr post-treatment) as depicted in **Figure 1**. Liver tissues were collected and frozen for microarray analysis (n=3 per time point per group). The tissues were lysed and homogenized using Trizol and the RNA was further purified and treated with DNase using RNeasy

columns (Qiagen). Then cRNA prepared from the RNA of liver tissues using protocols provided by Affymetrix were utilized to hybridize Rat Genome 230 2.0 Array (GeneChip, Affymetrix) comprised of more than 31,000 probe sets.

RT-PCR analysis

qPCR gene expression studies were performed using TaqMan gene expression assays. A detailed description of the methods can be found in the supplementary materials. The

Microarray analysis in liver following burn and CLP

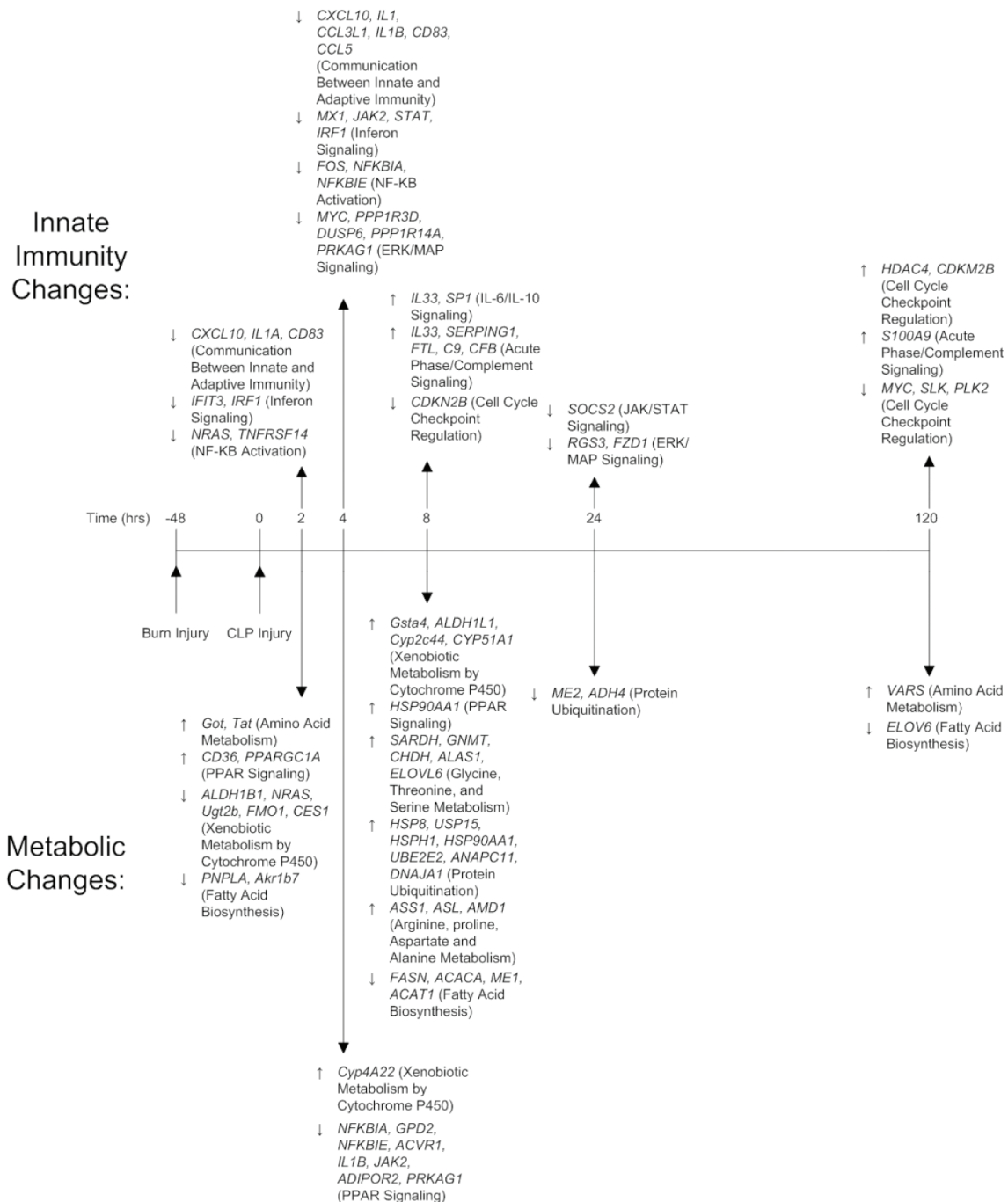


Figure 2. Key Metabolic and Immune Genes Over Time. Genes were identified first by Stastical Analysis of Microarrays (SAM), and then by pathway analysis through IPA. Genes related to transcriptional regulation of immune function, and cytokine signaling can be found down regulated by hour 4, and up regulated by hour 8. Metabolic functions related to amino acid catabolism are up regulated early relative to carbon metabolic pathways, while xenobiotic metabolism follows similar patterns to immune signaling genes.

expression level of the housekeeping gene GADPH [16] was used as an internal reference, and all fold changes are displayed as comparisons between BCLP and SCLP levels of the gene at each time point.

Data analysis

Genome expression data analysis was accomplished through pairwise comparisons between the burn+CLP (BCLP) and sham burn+CLP SCLP

Microarray analysis in liver following burn and CLP

Table 1. Genes that show significant fold change following burn priming when compared with CLP within key metabolic and immune pathways. All listed genes were identified by SAM to be significantly different between both conditions, and in agglomerate found by IPA to be significant in their associated pathways

Immune Function	
Pathways	Genes
Communication between Adaptive and Innate Immunity	<i>Cxcl10, Il1a, Il1, Ccl311/Ccl313, Il1b, Cd83 and Ccl5</i>
Interferon Signaling	<i>Ifit3, Mx1, Jak2, Stat and Irf1</i>
NF-KB Activation	<i>Nra, Tnfrsf14, Fos, Nfkbia and Nf</i>
IL-6/IL-10 Signaling	<i>Fos, Il1a, Nfkbia, Nfkbie, Il1b and Jak2</i>
ERK/MAP Signaling	<i>Myc, Ppp1r3d, Dusp6, Ppp1r14a and Prkag1</i>
JAK/STAT Signaling	<i>Cish and Socs2</i>
RXR Activation	<i>Cyp2b6 and Cd36</i>
Acute Phase Response Signaling/Complement Signaling	<i>Il33, Serping1, Ftl, C9, Cfb and S100a9</i>
Cell Cycle Check Point Regulation	<i>Cdkn1b, Hdac4, Cdkn2b, Myc, Slk and Plk2</i>
Metabolic Function	
Pathways	Genes
PPAR- γ Signaling	<i>Cd36, Ppargc1a, Nfkbia, Gpd2, Nfkbie, Acvr1, Il1b, Jak2, Adipor2 and Prkag1</i>
Xenobiotic Metabolism	<i>Aldh1b1, Nras, Ugt2b, Fmo1, Ces1, Cyp4a22, Gsta4, Aldh1l1, and Cyp51a1</i>
Pyruvate/Propanoate Metabolism	<i>Aldh1b1, Hk2, Pklr and Pfkf</i>
Glycine, Threonine, and Serine Metabolism	<i>Sardh, Gmmt, Chdh, Alas1 and Elov6</i>
Arginine, Proline, Aspartate and Alanine Metabolism	<i>Ass1, Asl, Amd1 and Prodh</i>
Amino Acid Metabolism	<i>Got, Tat, Aox1 and Vars</i>
Fatty Acid Biosynthesis	<i>Pnpla, Akr1b7, Fasn, Acaca, Mel, Acat1, and Elov6</i>
Protein Ubiquitination	<i>Hspa8, Usp15, Hsph1, Hsp90aa1, Ube2e2, Anapc11, Dnaj1, Me2 and Adh4</i>
NRF2 Mediated Oxidative Stress Response	<i>Sod2 and Gstm3</i>

groups at each time point. DNA chip analyzer (dChip) software [17] was used with invariant-set normalization and perfect match (PM) model to generate expression values. In order to characterize the probesets which show significant fold change at each time point, the method of statistical analysis of microarrays (SAM) was used [14]. This method compares the gene expression of the two response variables, BCLP and SCLP. Briefly, by computing a statistic g_i for each gene i , the strength of the relationship between the response variable (BCLP) and the standard (SCLP) is measured. False discovery is controlled via the random permutation of the gene response sets, in order to calculate the probability that the observed response is statistically significant. Following this, we characterize the biological relevance of the genes found to be statistically significant through SAM by evaluating the enrichment of the corresponding subsets in circadian rhythm specific pathways using the pathway enrichment function ($p < 0.05$) in Ingenuity Pathway Analysis (IPA) tools (Ingenuity Systems, Mountain View, CA) as well as analyzing the functions of individual genes extensively. For the analysis of the RT-PCR results, averaged normalized data for each experimental

gene was compared between BCLP groups and SCLP groups using the $2^{-\Delta\Delta C_t}$ method [18].

Results

Identification of BCLP related patterns and characterization of per day changes

Hepatic gene expression levels were measured 2, 4, 8, 12, 16, 20, 24, 48, 120 and 168 hours following BCLP and SCLP treatment. Differences in gene expression in BCLP, when compared to SCLP, were identified at each time point. The complete list of genes identified can be found in [Supplementary Table 2](#) described as up regulated or down regulated categories, relative to SCLP. Interestingly, for time points 16, 20, 48, and 168 hours post-injury, no significant gene expression differences were identified indicating identical gene expression between the BCLP and SCLP conditions for those time points. The full list of genes which passed IPA pathway analysis with p values less than .05 are shown in [Supplementary Table 1](#) along with their specific IPA identified pathways. The most relevant to innate immunity and hepatic metabolism following injury are summarized below, and in [Table 1](#).

Innate immunity related pathways

Over the 7 days post injury, 9 total pathways related to innate immunity showed significant changes in expression between BCLP and SCLP, indicating a change in transcriptional output between the two injuries. Specific genes associated with these pathways can be found in **Table 1**. Pathways which were down regulated in the first four hours include Communication between Adaptive and Innate Immune Systems, Interferon Signaling and NF- κ B activation, which all correspond to key cytokines and intracellular proteins that recognize and propagate the inflammatory response. The IL-6/IL-10 Signaling pathway, related to the activity of key pro inflammatory cytokines, had similar dynamics, but remained suppressed 4 hours longer than previous pathways. The ERK/MAP signaling pathway, associated with G protein activation of the immune response, was similarly suppressed early, but also showed suppression at one day post injury. The JAK/STAT signaling pathway, associated in this case with suppression of cytokine signaling, does not follow a similar regulatory pattern, but is instead suppressed halfway through the first day. In addition, the chemokine receptor related pathway called RXR Activation was elevated midway through the first day as well. The acute phase response signaling/complement signaling pathway, associated with anti bacterial acute phase protein production, was activated both early in the time course, but also very late, at 5 days post injury. The final pathway is associated with Cell Cycle Check Point Regulation, which controls cell proliferation both during the immune response, and shows similar patterns to the complement signaling pathway, with early suppression of anti proliferators in the first day of injury, and late activation of anti proliferators on the fifth day of injury. Overall, significant activity is observed very early in the time course, as well as at the first day, and the fifth day marks.

Metabolism related pathways

In addition to pathways associated with innate immunity, 9 pathways related to hepatic metabolic changes showed significant changes following injury in BCLP compared to SCLP over a 7 day time course. Specific genes associated with these pathways can be found in **Table 1**. Pathways with heavy activity early in the time

course include PPAR- γ Signaling and Xenobiotic Metabolism, which both are metabolic functions that crosstalk with innate immunity to degrade foreign bodies, and are activated early, then suppressed, or suppressed and then activated, respectively. Pyruvate/Propanoate Metabolism is a pathway critical to central carbon metabolism which is suppressed over the first four hours of injury. Specific amino acid pathways related to Glycine, Threonine, and Serine Metabolism and Arginine, Proline, Aspartate and Alanine Metabolism are activated 8 hours post injury, and in the case of the latter, persist to 12 hours post injury, at a time when previous pathways are winding down in activity. More general pathways related to Amino Acid Metabolism (including branched chain amino acid activity) were consistently activated early in the time course, and again as late as 5 days post injury, while the Fatty Acid Biosynthesis pathway is suppressed at those same time points. The Protein Ubiquitination pathway, which is related to the catabolism of proteins into their component amino acids, was activated by 8 hours post injury, but then suppressed at 24 hours post injury. The final metabolic pathway observed is related to NRF2 Mediated Oxidative Stress Response, which shows suppression midway through the first day, and whose functions primarily relate to the scavenging of potentially damaging reactive oxygen species within the cell. Similar to the innate immune pathways, genes associated with metabolic function appear to show activity early in the time course, or later, at 1 day or 5 days post injury.

RT-PCR confirmation of expression levels

In order to confirm the experimental microarray results, select genes were chosen for RT-PCR analysis that had passed both the SAMS tests and the false positive tests, and were significant biologically in the context of observed pathways. The full list of genes that were selected are *Slc1a4*, *Angptl4*, *Pcolce*, *Nfkb1a*, *Stam2* and *G6pd*, which were up and down regulated at 2, 4 and 168 hours respectively. *Slc1a4* and *G6pd* are metabolic genes that are responsible for producing proteins responsible for amino acid transport into the cell, and central carbon metabolism respectively, while *Angptl4* and *Pcolce* are genes that encode acute phase proteins produced by the liver. *Nfkb1a* is a component of the NF- κ B transcription factor, which is

Microarray analysis in liver following burn and CLP

Table 2. RTPCR Confirmation of Affymetrix Gene Expression Fold Change. Above are shown the 6 genes that were selected for RT-PCR confirmation: mean fold change compares the average BCLP expression levels to those of the SCLP condition, in both the microarray and the RT-PCR

Time	Gene Symbol	Gene Name	Mean Fold Change	
			Affymetrix	RTPCR
2h post CLP	Slc1a4	Solute carrier family 1 (glutamate/neutral amino acid transporter), member 4	2.69	3.47
	Angptl4	Angiopoietin-like 4	0.33	0.36
4h post CLP	Pcolce	Procollagen C-endopeptidase enhancer	3.05	6.43
	Nfkbia	Nuclear factor of kappa light polypeptide gene enhancer in B-cells inhibitor, alpha	0.49	0.77
Day 7 post CLP	Stam2	Signal transducing adaptor molecule (SH3 domain and ITAM motif) 2	2.49	1.07
	G6pd	Glucose-6-phosphate dehydrogenase	0.42	0.54

well known for its activity in acute inflammation, and *Stam2* is a component of a downstream cytokine receptor signaling pathway. These genes reinforce trends, for example, RT-PCR results for *Nfkbia*, and *G6pd*, which encode a sub unit of the critical immune response transcription factor NF-KB and central carbon metabolism through Glucose-6-phosphate dehydrogenase respectively, lend significant weight to the more general observations of immune suppression and lowered carbon based metabolic activity. The results are shown in **Table 2**, where the trends in fold change match between the microarray experimental data and the RT-PCR data in every case, although the magnitude of the fold changes sometimes differs between the two experimental methods.

Discussion

While the innate immune system usually responds to systemic threats with both pro inflammatory and anti inflammatory phases [6], recent evidence suggests that the magnitude of the inflammatory response is highly dependent on the status of the host at the time of injury [19]. Because inflammatory outcomes differ significantly between patients [20], it is necessary to understand how prior injuries that alter the innate immune system, such as burn [9], influence the progression of the inflammatory response during sepsis. In the experimental design outlined in **Figure 1**, we utilized rat model of thermal injury, which we have shown in previous works to induce an immunosuppressive state at 16 hours post injury that continues to be persistent past the 24 hour mark

[21] and assessed its effects on a subsequent septic insult.

The effect of burn priming on immune function

In previous work [15], we identified key motifs in the short term liver response of rodents to CLP when compared to uninjured animals, including a predominantly pro inflammatory cluster, with multiple cytokines, cytokine signals, complement, and coagulation proteins consistently upregulated. Therefore, fold changes observed between Burn-CLP animals and CLP animals represent deviations from this acute pro inflammatory trend. These changes are summarized in the top half of **Figure 2**, which shows key genes involved in Innate Immune pathways which are altered during the time course. During the first 4 hours after the septic insult, many of the immune regulated genes were suppressed under BCLP compared to SCLP. These genes are primarily involved in cytokine production, NF-κB signaling, and innate and adaptive communication through chemokines and other motifs. The suppression appears to be significantly stronger at the 4 hour time point, with critical inflammatory genes suppression (including *IL1*, *STAT1*, and *JAK2*) after thermal priming. In contrast the subsequent 4 hours post injury (the 8 hour time point) show significant up regulation of the immune system including several cytokines such as IL-33, a known Th2 cell attractor [22]. Further, at this time point, proinflammatory complement proteins (anti-bacterial acute phase reactants), are elevated in contrast with the suppression of inflammatory mediators observed previously. The observed early sup-

pression of pro inflammatory functions is likely caused by the burn priming: in single injury animals, burn injuries caused the animal to enter an immunosuppressive state during the first 24 hours, which would potentially dampen the acute response to CLP. This suppression gives way to an overshoot of pro inflammatory mediators not long after, indicating that burn does not promote pro or anti inflammatory mediators, but instead disrupts the balance between both in the healthy CLP response. In this case, this "spring back" of pro inflammatory mediators is dampened back down to a normal CLP response before 24 hours, however, in a more severe injury, the first 8 hours may represent a critical time period where an overshoot may overwhelm anti inflammatory forces that are designed to counterbalance it.

In previous studies, we have compared the hepatic response to single injuries that involved a surgical trauma with septic complications (CLP), to a surgical trauma that did not have septic complications (sham-CLP: a procedure involving the same incisions, but with no puncture of the cecum), and discovered that these injuries, despite their similarities, provoked huge differences in the hepatic response over the short and long term [10]. In contrast to those results, the temporal nature of the burn priming of CLP appears to affect the strength of the pro inflammatory and anti inflammatory stimuli, rather than shifting the dynamic entirely. While there is early immune suppression relative to the CLP condition, the number of genes observed as suppressed that have innate immune functions in the burn-CLP case are much smaller than the size of the pro inflammatory clusters observed in the single injury CLP results, and thus, the observed trend is more a dampening of the acute pro inflammatory CLP response, as opposed to an immune suppressive response.

Furthermore, although acute phase protein production and cytokine production have been analyzed together in innate immune function due to their common functionalities, they are traditionally produced by heterogeneous cell types in the liver, which cannot differentiate. Though it is most likely that acute phase protein production originates from hepatocytes, while cytokine production originates from

Kupffer cells, further investigations are required to understand how these cells communicate between one another to produce the observed response.

The effect of burn priming on metabolism

Our previous work on the short-term metabolic response following CLP indicates that the induced sepsis is associated with a shift toward increased metabolism via central carbon metabolism, fatty acid metabolism, and amino acid metabolism [15]. In contrast, the priming of the burn injury does not appear to increase net metabolism, but instead shifts the emphasis of consumed metabolites towards nitrogen based sources. This can be observed through the bottom half of **Figure 2**, which shows key genes related to metabolic enzymes involved in nitrogen metabolism, fatty acid metabolism, and oxidative stress. Almost immediately following CLP injury, we observed significant differences in metabolic response in burn-primed animals compared to the unprimed CLP group, particularly with respect to amino acid metabolism. Genes associated with amino acid metabolism are up regulated over the first 8 hours following injury, and then return to normal. Furthermore, the up regulation of amino acid degradation coincides with a down regulation of fatty acid energy sources, indicating that the burn injury predisposes the host to utilize an amino acid based energy source for the acute phase response. Given that amino acid degradation, through the urea cycle, is the primary mechanism by which the liver enters a negative nitrogen balance [23], this metabolic shift can be characterized as a move towards a state of hypermetabolism following burn injury, despite a suppressed immune response. Interestingly, there is no indication in our previous works that the single burn injury shifts metabolism towards nitrogen sources at the expense of carbon based energy [12]. The phenomenon of an energy shift towards amino acids is remarkably different from the single injuries, which simply increase metabolic activity through multiple channels, and bears further investigation.

In addition to catabolic changes, xenobiotic metabolism continued to increase over the first 8 hours following injury, while NRF2 mediated-oxidative responses were down regulated. A

similar increase in xenobiotic metabolism is also observed halfway through the first day, corresponding to moderately increased in immune function. This implies that systemic oxidation is higher post burn at this time point than seen with CLP alone, though to what degree remains unknown. Our previous characterizations of the hepatic response following CLP as a single injury [11] have also linked xenobiotic metabolism through cytochrome P450 to inflammation, indicating that this metabolic pathway is at least partially co-regulated with innate immunity. It is not clear how interconnected these elements of xenobiotic metabolism are with other metabolic pathways within hepatocytes, but their communication may represent an important link between inflammatory signaling elements and energy regulation that has hitherto been overlooked.

The effect of burn priming on the long term response

One of the interesting observations that came out of our previous work on the long term effects of CLP in a single injury model was the emergence of significant anti inflammatory gene expression at the 5 day mark, which occurred following a return to baseline at day 2 [24]. Interestingly, while most of the long term data points show no difference following burn priming, activity at the 5-day mark does occur, indicating that there is “memory” of the burn injury that persists through into the long term recovery response for CLP. Observed gene changes in this peak following burn priming include the activation of further wound repair, the down regulation of fatty acid synthesis, and the up regulation of amino acid synthesis. The preference for amino acid synthesis over fatty acid synthesis in the long term is likely the direct result of burn injury priming: creating a preference for amino acid *degradation* at the expense of lipid degradation in the short term response. These findings may be compensatory for relatively larger loss of amino acids in the early phase leading to increased synthesis later. None of the observed genes indicate a suppression of the anti inflammatory wound healing response, and to the contrary, they appear to enhance it. Due to the scarcity of data around this point, further investigations centering around 5 days post injury would be required to understand whether the wound

healing response observed at this time point is persistent, and whether it is a mechanistic function of burn, or just indicative of increased injury to be repaired.

Conclusion

Using high throughput functional genomic techniques, we are able to compare previous data from single injury models of both burn and sepsis with a combined double hit model of the injury in order to understand the mechanisms by which disparate injuries might combine to create a response more severe than the sum of its parts. The priming with thermal injury before CLP creates an early immune suppression characteristic of the burn injury, followed by a resurgent inflammatory response that overshoots the baseline CLP response through a “spring back” mechanism. Pathways critical to this mechanism include NF-KB activation, IL-6/IL-10 signaling, acute phase response signaling, and communication between the adaptive and innate immune systems. Further, priming with thermal injury exacerbates post-CLP hypermetabolism through significantly increased amino acid catabolism at the expense of carbon catabolism through pyruvate and fatty acid metabolism pathways, a phenomenon unique to the double hit injury, while xenobiotic metabolism appears to be closely linked with immune functions. This indicates that excess urea production associated with amino acid degradation may be a byproduct of this metabolic shift which involves pathways not observed in the clinical pathologies. Further, we identify that the 5 day long term response, previously identified as critical in single injuries, remains a hitherto unexplored point of resurgent gene expression that promotes wound healing and an immune suppressive state over the long term. Thus the immune suppressive state imposed by burn creates a more severe acute CLP response that has potentially severe metabolic and inflammatory effects, which appear to be partially co-regulated. Mitigating this immune suppression from burn may therefore be a viable clinical intervention for burn-sepsis related pathologies.

Acknowledgements

The authors gratefully acknowledge the financial support from NIH grant GM082974.

Funding

National Institute of Health (NIH) GM082974.

Subject category

Shock /Sepsis/Trauma/Critical Care.

Address correspondence to: Ioannis P Androulakis, Biomedical Engineering, Rutgers University, 599 Taylor Road, Piscataway, NJ 08854. Tel: 732-445-4500 x612; Fax: 732-445-3753; E-mail: yannis@rci.rutgers.edu

References

[1] Fitzwater J, Purdue GF, Hunt JL and O'Keefe GE. The risk factors and time course of sepsis and organ dysfunction after burn trauma. *J Trauma* 2003; 54: 959-966.

[2] Moss NM, Gough DB, Jordan AL, Grbic JT, Wood JJ, Rodrick ML and Mannick JA. Temporal correlation of impaired immune response after thermal injury with susceptibility to infection in a murine model. *Surgery* 1988; 104: 882-887.

[3] Schwacha MG, Schneider CP and Chaudry IH. Differential expression and tissue compartmentalization of the inflammatory response following thermal injury. *Cytokine* 2002; 17: 266-274.

[4] Adib-Conquy M and Cavailon JM. Compensatory anti-inflammatory response syndrome. *Thromb Haemost* 2009; 101: 36-47.

[5] Deitch EA. Multiple organ failure. Pathophysiology and potential future therapy. *Ann Surg* 1992; 216: 117-134.

[6] Hotchkiss RS, Coopersmith CM, McDunn JE and Ferguson TA. The sepsis seesaw: tilting toward immunosuppression. *Nat Med* 2009; 15: 496-497.

[7] Jaeschke H. Reactive oxygen and mechanisms of inflammatory liver injury: Present concepts. *J Gastroenterol Hepatol* 2011; 26 Suppl 1: 173-179.

[8] Wu RQ, Xu YX, Song XH, Chen LJ and Meng XJ. Adhesion molecule and proinflammatory cytokine gene expression in hepatic sinusoidal endothelial cells following cecal ligation and puncture. *World J Gastroenterol* 2001; 7: 128-130.

[9] DeJager L, Pinheiro I, Dejonckheere E and Libert C. Cecal ligation and puncture: the gold standard model for polymicrobial sepsis? *Trends Microbiol* 2011; 19: 198-208.

[10] Mattick JS, Yang Q, Orman MA, Ierapetritou MG, Berthiaume F and Androulakis IP. Long-

term gene expression profile dynamics following cecal ligation and puncture in the rat. *J Surg Res* 2012; 178: 431-442.

[11] Yang Q, Mattick JS, Orman MA, Nguyen TT, Ierapetritou MG, Berthiaume F and Androulakis IP. Dynamics of Hepatic Gene Expression Profile in a Rat Cecal Ligation and Puncture Model. *J Surg Res* 2012 Aug; 176: 583-600.

[12] Yang Q, Orman MA, Berthiaume F, Ierapetritou MG and Androulakis IP. Dynamics of short-term gene expression profiling in liver following thermal injury. *J Surg Res* 2011; 176: 549-558.

[13] Akira S and Takeda K. Toll-like receptor signaling. *Nat Rev Immunol* 2004; 4: 499-511.

[14] Tusher VG, Tibshirani R and Chu G. Significance analysis of microarrays applied to the ionizing radiation response. *Proc Natl Acad Sci U S A* 2001 Apr 24; 98: 5116-21. Epub 2001 Apr 17.

[15] Yang Q, Mattick JS, Orman MA, Nguyen TT, Ierapetritou MG, Berthiaume F and Androulakis IP. Dynamics of hepatic gene expression profile in a rat cecal ligation and puncture model. *J Surg Res* 2012; 176: 583-600.

[16] Barber RD, Harmer DW, Coleman RA and Clark BJ. GAPDH as a housekeeping gene: analysis of GAPDH mRNA expression in a panel of 72 human tissues. *Physiol Genomics* 2005 May 11; 21: 389-95.

[17] Li C and Wong WH. Model-based analysis of oligonucleotide arrays: expression index computation and outlier detection. *Proc Natl Acad Sci U S A* 2001; 98: 31-36.

[18] Livak KJ and Schmittgen TD. Analysis of relative gene expression data using real-time quantitative PCR and the 2⁻(Delta Delta C(T)) Method. *Methods* 2001; 25: 402-408.

[19] Castanon-Cervantes O, Wu M, Ehlen JC, Paul K, Gamble KL, Johnson RL, Besing RC, Menaker M, Gewirtz AT and Davidson AJ. Dysregulation of Inflammatory Responses by Chronic Circadian Disruption. *The Journal of Immunology* 2010; 185: 5796-5805.

[20] Weycker D, Akhras KS, Edelsberg J, Angus DC and Oster G. Long-term mortality and medical care charges in patients with severe sepsis. *Critical Care Med* 2003 Sep; 31: 2316-23.

[21] Yang Q, Orman MA, Berthiaume F, Ierapetritou MG and Androulakis IP. Dynamics of short-term gene expression profiling in liver following thermal injury. *J Surg Res* 2012; 176: 549-558.

[22] Komai-Koma M, Xu D, Li Y, McKenzie ANJ, McInnes IB and Liew FY. IL-33 is a chemoattractant for human Th2 cells. *Eur J Immunol* 2007 Oct; 37: 2779-86.

Microarray analysis in liver following burn and CLP

- [23] Kamin H and Handler P. The metabolism of parenterally administered amino acids. II. Urea synthesis. *J Biol Chem* 1951; 188: 193-205.
- [24] Mattick JS, Yang Q, Orman MA, Ierapetritou MG, Berthiaume F and Androulakis IP. Long-term gene expression profile dynamics following cecal ligation and puncture in the rat. *J Surg Res* 2012 Nov; 178: 431-42.

Microarray analysis in liver following burn and CLP

Supplementary materials

Quantitative real-time PCR

qPCR gene expression studies were performed for genes of interest (GOI) as validation of the microarray results. The RNA samples were amplified with Nugen WT Pico Kit (Part# 3300-A01) (NuGEN Technologies Inc, San Carlos, CA, USA). RNA was reversed transcribed into DNA. Then cDNA samples were diluted by 100 times. All the samples were tested in triplicates. qPCR was performed using the ABI 7900 HT Sequence Sequence Detection System (TaqMan; Applied Biosystems, Foster City, CA, USA) using standard fluorescent chemistries and thermal cycling conditions. Primer and probe sequences were designed for each experimental gene's mRNA sequence using Primer Express software (Applied Biosystems) as shown in **Table 3**. For the gene of interest, 6-10 ng of cDNA was mixed with 20 μ M FWR/Rvse and 10 μ M (UPL) Probe (UPL). The reference gene GAPDH was added into Rodent GAPDH control kit ABI (Part No.4308313) (TaqMan; Applied Biosystems, Foster City, CA, USA) with 10 μ M FWR/Rvse and 20 μ M Probe. Thermal cycling conditions were as specified by the manufacturer: 50°C for 2 min, 95°C for 10 min, and 40 cycles as follows: 95°C for 15 s, ramp to 60°C for 1 min.

Analysis of qPCR data

For the analysis of the qPCR results, averaged normalized data for each experimental gene was compared between B_CLP groups and SB_CLP groups using the $2^{-\Delta\Delta C_t}$ method.

Microarray analysis in liver following burn and CLP

Supplementary Table 1. Full Pathway Analysis By IPA of Genes With Significant Fold Change Between BCLP and SCLP Conditions

Time (hr)	Up/Down Regulation	Pathway	Gene Annotation	p-value
2	Up	Phenylalanine, Tyrosine and Tryptophan Biosynthesis	<i>Got1, Tat</i>	0.000398
2	Up	Circadian Rhythm Signaling	<i>Per1, Cry2</i>	0.001318
2	Up	Phenylalanine Metabolism	<i>Got1, Tat</i>	0.002089
2	Up	Tyrosine Metabolism	<i>Got1, Tat</i>	0.007244
2	Up	PPAR Signaling	<i>Cited2, Ppargc1A</i>	0.012303
2	Up	Glycerophospholipid Metabolism	<i>Etnk1, Got1</i>	0.019055
2	Up	PPAR α /RXR α Activation	<i>Cd36, Ppargc1A</i>	0.034674
2	Up	RAR Activation	<i>Cited2, Ppargc1A</i>	0.035481
2	Down	Xenobiotic Metabolism Signaling	<i>Aldh1B1, Il1A, Nras, Ugt2B, Fmo1, Ces1</i>	0.00138
2	Down	Role of MAPK Signaling in the Pathogenesis of Influenza	<i>Cxcl10, Nras, Pnpla3</i>	0.002399
2	Down	Communication between Innate and Adaptive Immune Cells	<i>Cxcl10, Il1A, Cd83</i>	0.006761
2	Down	Atherosclerosis Signaling	<i>Il1A, Pnpla3, Tnfrsf14</i>	0.007413
2	Down	Interferon Signaling	<i>Ifit3, Irf1</i>	0.00912
2	Down	Glycerolipid Metabolism	<i>Aldh1B1, Pnpla3, Akr1B7</i>	0.009333
2	Down	Pentose and Glucuronate Interconversions	<i>Ugt2B, Akr1B7</i>	0.012303
2	Down	Thyroid Cancer Signaling	<i>Cxcl10, Nras</i>	0.014791
2	Down	Role of Hypercytokinemia/hyperchemokine in the Pathogenesis of Influenza	<i>Cxcl10, Il1A</i>	0.014791
2	Down	Bile Acid Biosynthesis	<i>Aldh1B1, Akr1C4</i>	0.022387
2	Down	Estrogen-Dependent Breast Cancer Signaling	<i>Nras, Akr1C4</i>	0.026303
2	Down	Activation of IRF by Cytosolic Pattern Recognition Receptors	<i>Dhx58, Isg15</i>	0.02884
2	Down	Pyruvate Metabolism	<i>Aldh1B1, Akr1B7</i>	0.032359
2	Down	Endothelin-1 Signaling	<i>Nras, Pnpla3, Casp4</i>	0.033113
2	Down	Aggrin Interactions at Neuromuscular Junction	<i>Nras, Utrn</i>	0.033113
2	Down	PPAR α /RXR α Activation	<i>Nras, Fasn, Ckap5</i>	0.034674
2	Down	IL-17 Signaling	<i>Cxcl10, Nras</i>	0.037154
2	Down	Pathogenesis of Multiple Sclerosis	<i>Cxcl10</i>	0.037154
2	Down	NF- κ B Activation by Viruses	<i>Nras, Tnfrsf14</i>	0.038019
2	Down	Prolactin Signaling	<i>Nras, Irf1</i>	0.038019
2	Down	LXR/RXR Activation	<i>Il1A, Fasn</i>	0.040738
2	Down	Fatty Acid Biosynthesis	<i>Fasn</i>	0.041687
2	Down	Androgen and Estrogen Metabolism	<i>Ugt2B, Akr1C4</i>	0.043652
4	Up	Arachidonic Acid Metabolism	<i>Cyp4A22</i>	0.021878
4	Up	Fatty Acid Metabolism	<i>Cyp4A22</i>	0.022387
4	Down	Glucocorticoid Receptor Signaling	<i>Icam1, Hspa14, Sgk1, Nfkbie, Jak2, Ccl5, Prkag1, Smarca4, Taf9B, Fos, Nfkbia, Il1B, Stat1</i>	0.0001
4	Down	Pathogenesis of Multiple Sclerosis	<i>Cxcl10, Ccl5, Cxcl11</i>	0.000224
4	Down	Role of PKR in Interferon Induction and Antiviral Response	<i>Tp53, Nfkbia, Nfkbie, Stat1, Irf1</i>	0.000245
4	Down	Production of Nitric Oxide and Reactive Oxygen Species in Macrophages	<i>Fos, Ppp1R3D, Nfkbia, Rnd3, Nfkbie, Ppp1R14A, Jak2, Stat1, Irf1</i>	0.000363
4	Down	IL-17A Signaling in Gastric Cells	<i>Cxcl10, Fos, Ccl5, Cxcl11</i>	0.000398
4	Down	Dendritic Cell Maturation	<i>Il1A, Icam1, Nfkbia, Nfkbie, Hla-Dqa1, Il1B, Cd83, Jak2, Stat1</i>	0.000479
4	Down	Prolactin Signaling	<i>Myc, Fos, Jak2, Prrr, Stat1, Irf1</i>	0.000603
4	Down	Colorectal Cancer Metastasis Signaling	<i>Tp53, Myc, Fos, Rnd3, Mmp15, Lrp6, Tcf7L1, Mmp2, Jak2, Stat1, Prkag1</i>	0.000646
4	Down	Aryl Hydrocarbon Receptor Signaling	<i>Tp53, Myc, Aldh1B1, Fos, Il1A, Il1B, Nfe2L2, Smarca4</i>	0.000776

Microarray analysis in liver following burn and CLP

4	Down	Type I Diabetes Mellitus Signaling	<i>Nfkbia, Nfkbie, Hla-Dqa1, Il1B, Jak2, Stat1, Irf1</i>	0.000933
4	Down	Role of BRCA1 in DNA Damage Response	<i>Tp53, Fancc, Stat1, Fancl, Smarca4</i>	0.001175
4	Down	Interferon Signaling	<i>Mx1, Jak2, Stat1, Irf1</i>	0.001318
4	Down	Role of Macrophages, Fibroblasts and Endothelial Cells in Rheumatoid Arthritis	<i>Myc, Fos, Il1A, Icam1, Nfkbia, Cebpd, Nfkbie, Lrp6, Il1B, Tcf7L1, Jak2, Ccl5</i>	0.001349
4	Down	IL-17A Signaling in Fibroblasts	<i>Fos, Nfkbia, Cebpd, Nfkbie</i>	0.001479
4	Down	Communication between Innate and Adaptive Immune Cells	<i>Cxcl10, Il1A, Ccl3L1/Ccl3L3, Il1B, Cd83, Ccl5</i>	0.001905
4	Down	Activation of IRF by Cytosolic Pattern Recognition Receptors	<i>Nfkbia, Nfkbie, Stat1, Adar, Isg15</i>	0.001995
4	Down	IL-6 Signaling	<i>Fos, Il1A, Nfkbia, Nfkbie, Il1B, Jak2</i>	0.002239
4	Down	Pyruvate Metabolism	<i>Aldh1B1, Pklr, Acat1, Acaca, Me1</i>	0.00263
4	Down	MIF Regulation of Innate Immunity	<i>Tp53, Fos, Nfkbia, Nfkbie</i>	0.002692
4	Down	IL-10 Signaling	<i>Fos, Il1A, Nfkbia, Nfkbie, Il1B</i>	0.002818
4	Down	PPAR α /RXR α Activation	<i>Nfkbia, Gpd2, Nfkbie, Acvr1, Il1B, Jak2, Adipor2, Prkag1</i>	0.002951
4	Down	Thyroid Cancer Signaling	<i>Cxcl10, Tp53, Myc, Tcf7L1</i>	0.003467
4	Down	Role of Hypercytokinemia/hyperchemokineemia in the Pathogenesis of Influenza	<i>Cxcl10, Il1A, Il1B, Ccl5</i>	0.003467
4	Down	Aminosugars Metabolism	<i>Hk2, Gnpda2, Nanp, Pde4B, Cyb561</i>	0.003631
4	Down	IL-15 Production	<i>Jak2, Stat1, Irf1</i>	0.007244
4	Down	TREM1 Signaling	<i>Icam1, Il1B, Cd83, Jak2</i>	0.007244
4	Down	Thrombopoietin Signaling	<i>Myc, Fos, Jak2, Stat1</i>	0.007762
4	Down	TNFR2 Signaling	<i>Fos, Nfkbia, Nfkbie</i>	0.007943
4	Down	Acute Phase Response Signaling	<i>Fos, Il1A, Sod2, Nfkbia, Nfkbie, Il1B, Jak2</i>	0.01
4	Down	IL-1 Signaling	<i>Fos, Il1A, Nfkbia, Nfkbie, Prkag1</i>	0.01
4	Down	Insulin Receptor Signaling	<i>Ppp1R3D, Sgk1, Ppp1R14A, Jak2, Ptpfr, Prkag1</i>	0.010715
4	Down	PPAR Signaling	<i>Fos, Il1A, Nfkbia, Nfkbie, Il1B</i>	0.012023
4	Down	Synthesis and Degradation of Ketone Bodies	<i>Bdh1, Acat1</i>	0.012023
4	Down	TWEAK Signaling	<i>Nfkbia, Nfkbie, Bag4</i>	0.012303
4	Down	CD40 Signaling	<i>Fos, Icam1, Nfkbia, Nfkbie</i>	0.012303
4	Down	Relaxin Signaling	<i>Fos, Gucy1B2, Nfkbia, Nfkbie, Pde4B, Prkag1</i>	0.012303
4	Down	Role of JAK2 in Hormone-like Cytokine Signaling	<i>Jak2, Prlr, Stat1</i>	0.013183
4	Down	Role of IL-17A in Psoriasis	<i>S100A9, S100A8</i>	0.014125
4	Down	Nitrogen Metabolism	<i>Ca3, Asns, Adar</i>	0.014454
4	Down	Hepatic Cholestasis	<i>Il1A, Tjp2, Nfkbia, Nfkbie, Il1B, Prkag1</i>	0.015136
4	Down	Hepatic Fibrosis / Hepatic Stellate Cell Activation	<i>Il1A, Icam1, Fgfr2, Il1B, Ccl5, Stat1</i>	0.015136
4	Down	Erythropoietin Signaling	<i>Fos, Nfkbia, Nfkbie, Jak2</i>	0.015136
4	Down	ERK/MAPK Signaling	<i>Myc, Fos, Ppp1R3D, Dusp6, Ppp1R14A, Stat1, Prkag1</i>	0.016596
4	Down	April Mediated Signaling	<i>Fos, Nfkbia, Nfkbie</i>	0.016596
4	Down	Small Cell Lung Cancer Signaling	<i>Tp53, Myc, Nfkbia, Nfkbie</i>	0.018621
4	Down	PDGF Signaling	<i>Myc, Fos, Jak2, Stat1</i>	0.018621
4	Down	B Cell Activating Factor Signaling	<i>Fos, Nfkbia, Nfkbie</i>	0.019055
4	Down	Renin-Angiotensin Signaling	<i>Fos, Jak2, Ccl5, Stat1, Prkag1</i>	0.019953
4	Down	Dopamine Receptor Signaling	<i>Ppp1R3D, Ddc, Ppp1R14A, Prkag1</i>	0.022909
4	Down	Type II Diabetes Mellitus Signaling	<i>Nfkbia, Pklr, Nfkbie, Adipor2, Prkag1</i>	0.024547
4	Down	Differential Regulation of Cytokine Production in Macrophages and T Helper Cells by IL-17A and IL-17F	<i>Il1B, Ccl5</i>	0.026303
4	Down	Graft-versus-Host Disease Signaling	<i>Il1A, Hla-Dqa1, Il1B</i>	0.027542
4	Down	Galactose Metabolism	<i>Hk2, B4Galt1, Pfkf</i>	0.02884
4	Down	TNFR1 Signaling	<i>Fos, Nfkbia, Nfkbie</i>	0.030903
4	Down	Wnt/ β -catenin Signaling	<i>Tp53, Myc, Axin2, Lrp6, Acvr1, Tcf7L1</i>	0.034674
4	Down	FXR/RXR Activation	<i>Il1A, Pklr, Foxa2, Il1B</i>	0.035481
4	Down	CDK5 Signaling	<i>Ppp1R3D, Egr1, Ppp1R14A, Prkag1</i>	0.035481
4	Down	CD27 Signaling in Lymphocytes	<i>Fos, Nfkbia, Nfkbie</i>	0.036308

Microarray analysis in liver following burn and CLP

4	Down	Role of Osteoblasts, Osteoclasts and Chondrocytes in Rheumatoid Arthritis	<i>Fos,Il1A,Nfkbia,Nfkbie,Lrp6,Il1B,Tcf7L1</i>	0.037154
4	Down	Bladder Cancer Signaling	<i>Tp53,Myc,Mmp15,Mmp24</i>	0.038019
4	Down	Differential Regulation of Cytokine Production in Intestinal Epithelial Cells by IL-17A and IL-17F	<i>Il1B,Ccl5</i>	0.038905
4	Down	Glycolysis/Gluconeogenesis	<i>Aldh1B1,Hk2,Pklr,Pfkm</i>	0.039811
4	Down	Cardiac β -adrenergic Signaling	<i>Akap13,PPP1R3D,PPP1R14A,Pde4B,Prkag1</i>	0.040738
4	Down	Role of IL-17A in Arthritis	<i>Nfkbia,Nfkbie,Ccl5</i>	0.041687
4	Down	Maturity Onset Diabetes of Young (MODY) Signaling	<i>Pklr,Foxa2</i>	0.041687
4	Down	NRF2-mediated Oxidative Stress Response	<i>Fos,Sod2,Dnajc4,Dnajc14,Fmo1,Nfe2L2</i>	0.043652
4	Down	HMGBl Signaling	<i>Fos,Il1A,Icam1,Rnd3</i>	0.045709
4	Down	Atherosclerosis Signaling	<i>Il1A,Icam1,Il1B,Tnfrsf14</i>	0.045709
4	Down	Role of JAK1, JAK2 and TYK2 in Interferon Signaling	<i>Jak2,Stat1</i>	0.045709
4	Down	Propanoate Metabolism	<i>Aldh1B1,Acat1,Acaca</i>	0.047863
4	Down	Role of JAK family kinases in IL-6-type Cytokine Signaling	<i>Jak2,Stat1</i>	0.048978
8	Up	Glycine, Serine and Threonine Metabolism	<i>Sardh,Gnmt,Chdh,Alas1,Elovl6</i>	4.79E-06
8	Up	Protein Ubiquitination Pathway	<i>Hspa8,Usp15,Hsph1,Hsp90Aa1,Ube2E2,Anapc11,Dnaja1</i>	3.39E-05
8	Up	Urea Cycle and Metabolism of Amino Groups	<i>Sardh,Ass1,Asl</i>	0.000186
8	Up	Complement System	<i>Serp1g1,C9,Cfb</i>	0.000204
8	Up	Acute Phase Response Signaling	<i>Il33,Serp1g1,Ftl,C9,Cfb</i>	0.000288
8	Up	Phenylalanine Metabolism	<i>Dhcr24,Aldh1L1,Elovl6</i>	0.000339
8	Up	Metabolism of Xenobiotics by Cytochrome P450	<i>Gsta4,Aldh1L1,Cyp2C44,Cyp51A1</i>	0.000692
8	Up	Aldosterone Signaling in Epithelial Cells	<i>Hspa8,Hsph1,Hsp90Aa1,Dnaja1</i>	0.001995
8	Up	Arginine and Proline Metabolism	<i>Ass1,Asl,Amd1</i>	0.002138
8	Up	One Carbon Pool by Folate	<i>Aldh1L1,Mthfd1</i>	0.002188
8	Up	Biosynthesis of Steroids	<i>Ebp,Hmgcr</i>	0.002399
8	Up	Methionine Metabolism	<i>Mat1A,Amd1</i>	0.004898
8	Up	Alanine and Aspartate Metabolism	<i>Ass1,Asl</i>	0.008128
8	Up	Tryptophan Metabolism	<i>Dhcr24,Cyp2C44,Cyp51A1</i>	0.010715
8	Up	Aryl Hydrocarbon Receptor Signaling	<i>Sp1,Aldh1L1,Hsp90Aa1</i>	0.012303
8	Up	Histidine Metabolism	<i>Aldh1L1,Elovl6</i>	0.013183
8	Up	Mitotic Roles of Polo-Like Kinase	<i>Hsp90Aa1,Anapc11</i>	0.019953
8	Up	Hypoxia Signaling in the Cardiovascular System	<i>Hsp90Aa1,Ube2E2</i>	0.022909
8	Up	IL-10 Signaling	<i>Il33,Sp1</i>	0.023442
8	Up	PXR/RXR Activation	<i>Abcb11,Alas1</i>	0.024547
8	Up	Aminosugars Metabolism	<i>Por,Sacm1L</i>	0.026303
8	Up	Tyrosine Metabolism	<i>Aldh1L1,Elovl6</i>	0.026915
8	Up	LXR/RXR Activation	<i>Il33,Hmgcr</i>	0.02884
8	Up	Linoleic Acid Metabolism	<i>Cyp2C44,Cyp51A1</i>	0.029512
8	Up	LPS/IL-1 Mediated Inhibition of RXR Function	<i>Abcb11,Aldh1L1,Alas1</i>	0.033113
8	Up	FXR/RXR Activation	<i>Il33,Abcb11</i>	0.037154
8	Up	PPAR Signaling	<i>Il33,Hsp90Aa1</i>	0.044668
8	Up	Nicotinate and Nicotinamide Metabolism	<i>Hipk1,Sacm1L</i>	0.047863
8	Down	Synthesis and Degradation of Ketone Bodies	<i>Acat1</i>	0.006457
8	Down	Antiproliferative Role of TOB in T Cell Signaling	<i>Cdkn1B</i>	0.014125
8	Down	Nitrogen Metabolism	<i>Ca3</i>	0.019498
8	Down	Cell Cycle: G1/S Checkpoint Regulation	<i>Cdkn1B</i>	0.0302
8	Down	Propanoate Metabolism	<i>Acat1</i>	0.0302
8	Down	Butanoate Metabolism	<i>Acat1</i>	0.032359
8	Down	Lysine Degradation	<i>Acat1</i>	0.033113
8	Down	Antiproliferative Role of Somatostatin Receptor 2	<i>Cdkn1B</i>	0.033884
8	Down	Pyruvate Metabolism	<i>Acat1</i>	0.035481
8	Down	Valine, Leucine and Isoleucine Degradation	<i>Acat1</i>	0.035481
8	Down	Small Cell Lung Cancer Signaling	<i>Cdkn1B</i>	0.038019
8	Down	HER-2 Signaling in Breast Cancer	<i>Cdkn1B</i>	0.040738

Microarray analysis in liver following burn and CLP

8	Down	VDR/RXR Activation	<i>Cdkn1B</i>	0.041687
8	Down	Cyclins and Cell Cycle Regulation	<i>Cdkn1B</i>	0.041687
8	Down	Prostate Cancer Signaling	<i>Cdkn1B</i>	0.042658
8	Down	Neuregulin Signaling	<i>Cdkn1B</i>	0.046774
12	Up	Tyrosine Metabolism	<i>Adh1C,Aox1</i>	0.000525
12	Up	Metabolism of Xenobiotics by Cytochrome P450	<i>Adh1C,Cyp2B6</i>	0.001288
12	Up	Fatty Acid Metabolism	<i>Adh1C,Cyp2B6</i>	0.001514
12	Up	Tryptophan Metabolism	<i>Aox1,Cyp2B6</i>	0.00166
12	Up	Inhibition of Angiogenesis by TSP1	<i>Cd36</i>	0.016218
12	Up	Retinol Metabolism	<i>Adh1C</i>	0.02138
12	Up	Bile Acid Biosynthesis	<i>Adh1C</i>	0.026303
12	Up	Valine, Leucine and Isoleucine Degradation	<i>Aox1</i>	0.031623
12	Up	PXR/RXR Activation	<i>Cyp2B6</i>	0.033113
12	Up	Arginine and Proline Metabolism	<i>Prodh</i>	0.034674
12	Up	LXR/RXR Activation	<i>Cd36</i>	0.036308
12	Up	Linoleic Acid Metabolism	<i>Cyp2B6</i>	0.036308
12	Up	FXR/RXR Activation	<i>Cyp8B1</i>	0.041687
12	Up	Glycolysis/Gluconeogenesis	<i>Adh1C</i>	0.042658
12	Up	Atherosclerosis Signaling	<i>Cd36</i>	0.044668
12	Up	Nicotinate and Nicotinamide Metabolism	<i>Aox1</i>	0.046774
12	Up	Glycerolipid Metabolism	<i>Adh1C</i>	0.048978
12	Down	NRF2-mediated Oxidative Stress Response	<i>Sod2,Gstm3</i>	0.001698
12	Down	Riboflavin Metabolism	<i>Acpp</i>	0.007244
12	Down	IL-9 Signaling	<i>Cish</i>	0.012303
12	Down	Neuroprotective Role of THOP1 in Alzheimer's Disease	<i>Hla-G</i>	0.014454
12	Down	Antigen Presentation Pathway	<i>Hla-G</i>	0.014454
12	Down	Graft-versus-Host Disease Signaling	<i>Hla-G</i>	0.016596
12	Down	Autoimmune Thyroid Disease Signaling	<i>Hla-G</i>	0.016982
12	Down	Glutathione Metabolism	<i>Gstm3</i>	0.02138
12	Down	JAK/Stat Signaling	<i>Cish</i>	0.021878
12	Down	GM-CSF Signaling	<i>Cish</i>	0.022387
12	Down	Cytotoxic T Lymphocyte-mediated Apoptosis of Target Cells	<i>Hla-G</i>	0.02884
12	Down	Allograft Rejection Signaling	<i>Hla-G</i>	0.029512
12	Down	OX40 Signaling Pathway	<i>Hla-G</i>	0.030903
12	Down	Crosstalk between Dendritic Cells and Natural Killer Cells	<i>Hla-G</i>	0.032359
12	Down	Communication between Innate and Adaptive Immune Cells	<i>Hla-G</i>	0.032359
12	Down	Type I Diabetes Mellitus Signaling	<i>Hla-G</i>	0.038905
12	Down	Metabolism of Xenobiotics by Cytochrome P450	<i>Gstm3</i>	0.040738
12	Down	Mitochondrial Dysfunction	<i>Sod2</i>	0.047863
12	Down	Aryl Hydrocarbon Receptor Signaling	<i>Gstm3</i>	0.048978
24	Down	Pyruvate Metabolism	<i>Me2,Adh4</i>	0.001413
24	Down	Lysine Biosynthesis	<i>Adh4</i>	0.009333
24	Down	IL-9 Signaling	<i>Socs2</i>	0.028184
24	Down	Role of JAK2 in Hormone-like Cytokine Signaling	<i>Socs2</i>	0.02884
24	Down	Nitrogen Metabolism	<i>Ca3</i>	0.0302
24	Down	Pentose and Glucuronate Interconversions	<i>Adh4</i>	0.033113
24	Down	Retinol Metabolism	<i>Adh4</i>	0.037154
24	Down	Galactose Metabolism	<i>Adh4</i>	0.038905
24	Down	Axonal Guidance Signaling	<i>Rgs3,Fzd1</i>	0.041687
24	Down	Fructose and Mannose Metabolism	<i>Adh4</i>	0.042658
24	Down	Bile Acid Biosynthesis	<i>Adh4</i>	0.045709
24	Down	JAK/Stat Signaling	<i>Socs2</i>	0.050119
120	Up	Cell Cycle: G1/S Checkpoint Regulation	<i>Hdac4,Cdkn2B</i>	0.014454
120	Up	Cyclins and Cell Cycle Regulation	<i>Hdac4,Cdkn2B</i>	0.027542

Microarray analysis in liver following burn and CLP

120	Up	Valine, Leucine and Isoleucine Biosynthesis	<i>Vars</i>	0.038019
120	Up	Role of IL-17A in Psoriasis	<i>S100A9</i>	0.041687
120	Down	Fatty Acid Biosynthesis	<i>Fasn,Acaca</i>	0.000214
120	Down	TR/RXR Activation	<i>Fasn,Acaca,Me1</i>	0.000891
120	Down	Mitotic Roles of Polo-Like Kinase	<i>Slk,Plk2</i>	0.008511
120	Down	Pyruvate Metabolism	<i>Acaca,Me1</i>	0.009772
120	Down	Tyrosine Metabolism	<i>Comt,Elov16</i>	0.011482
120	Down	LXR/RXR Activation	<i>Fasn,Acaca</i>	0.012589
120	Down	Dopamine Receptor Signaling	<i>Comt,PPP1R3C</i>	0.012589
120	Down	Glycerophospholipid Metabolism	<i>Bche,Elov16</i>	0.0302
120	Down	DNA Double-Strand Break Repair by Homologous Recombination	<i>Gen1</i>	0.030903
120	Down	AMPK Signaling	<i>Fasn,Acaca</i>	0.036308
120	Down	Polyamine Regulation in Colon Cancer	<i>Myc</i>	0.047863

Microarray analysis in liver following burn and CLP

Supplementary Table 2. Total Number of Genes Identified as Significantly Different via SAM

Number of Genes Identified by SAM at each time point

	2h	4h	8h	12h	16h	20h	24h	48 hr	120 hr	196 hr
Up regulation	45	9	82	10	0	0	0	0	107	0
Down regulation	144	426	15	11	0	0	35	0	73	0